Supplementary Materials

In vitro spectroscopy-based profiling of urothelial carcinoma: A Fourier transform Infrared and Raman imaging study

Monika Kujdowicz[1,2], Wojciech Placha[3], Brygida Mech[2], Karolina Chrabaszcz[2], Krzysztof Okoń[1] and Kamilla Malek [2,*]

[1] Department of Pathology, Faculty of Medicine, Jagiellonian University Medical College, Krakow, Grzegorzecka 16, 31-531, Poland

[2] Faculty of Chemistry, Jagiellonian University in Krakow, Krakow, Gronostajowa 2, 30-387, Poland

[3] Chair of Medical Biochemistry, Faculty of Medicine, Jagiellonian University Medical College, Krakow, Kopernika 7, 31-034, Poland

* Correspondence: kamilla.malek@uj.edu.pl

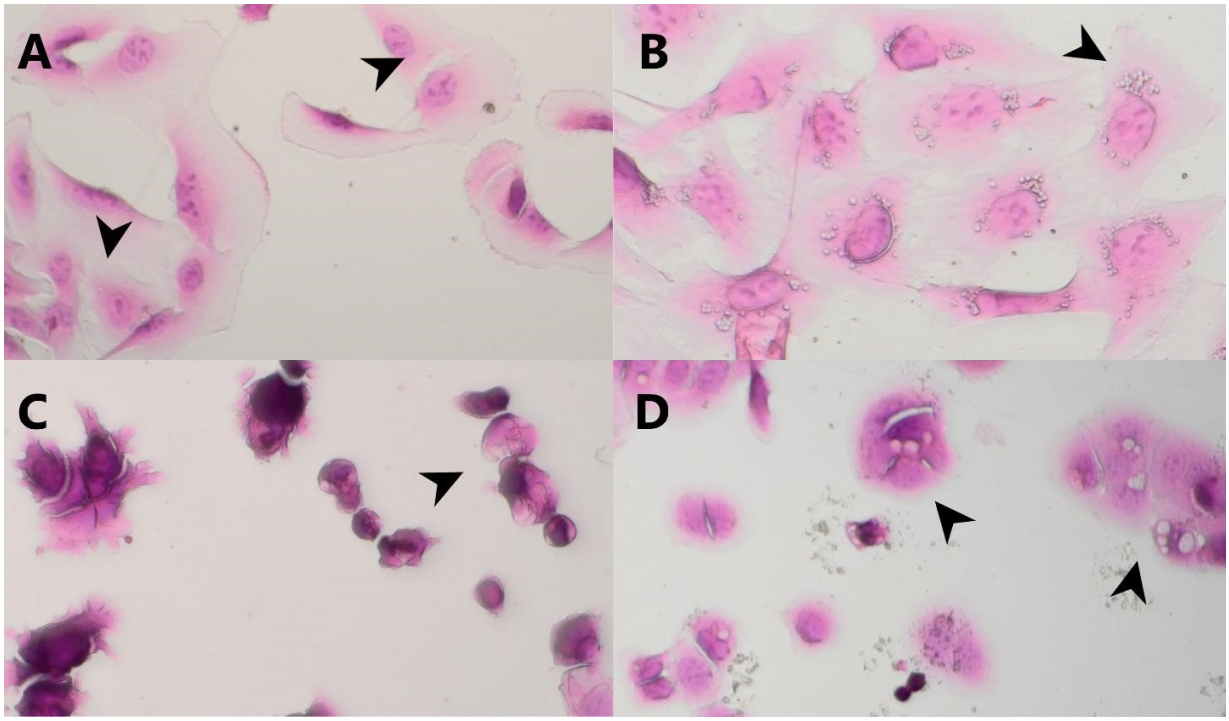

Figure S1. Enlarged images of HE stained HE cell lines containing cellular structures similar to graininess (arrowheads): A- T24a, B – T24p, C – RT4, D – HT-1376; magnification 200x.

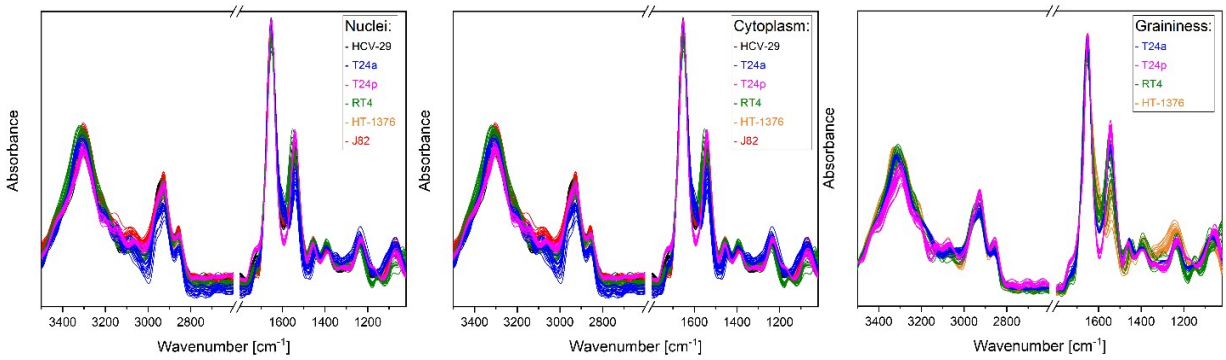

Figure S2. HD-FTIR spectra of nuclei, cytoplasm and graininess spectra (N = 20 per cell line) derived from UHCA analysis of single cells.

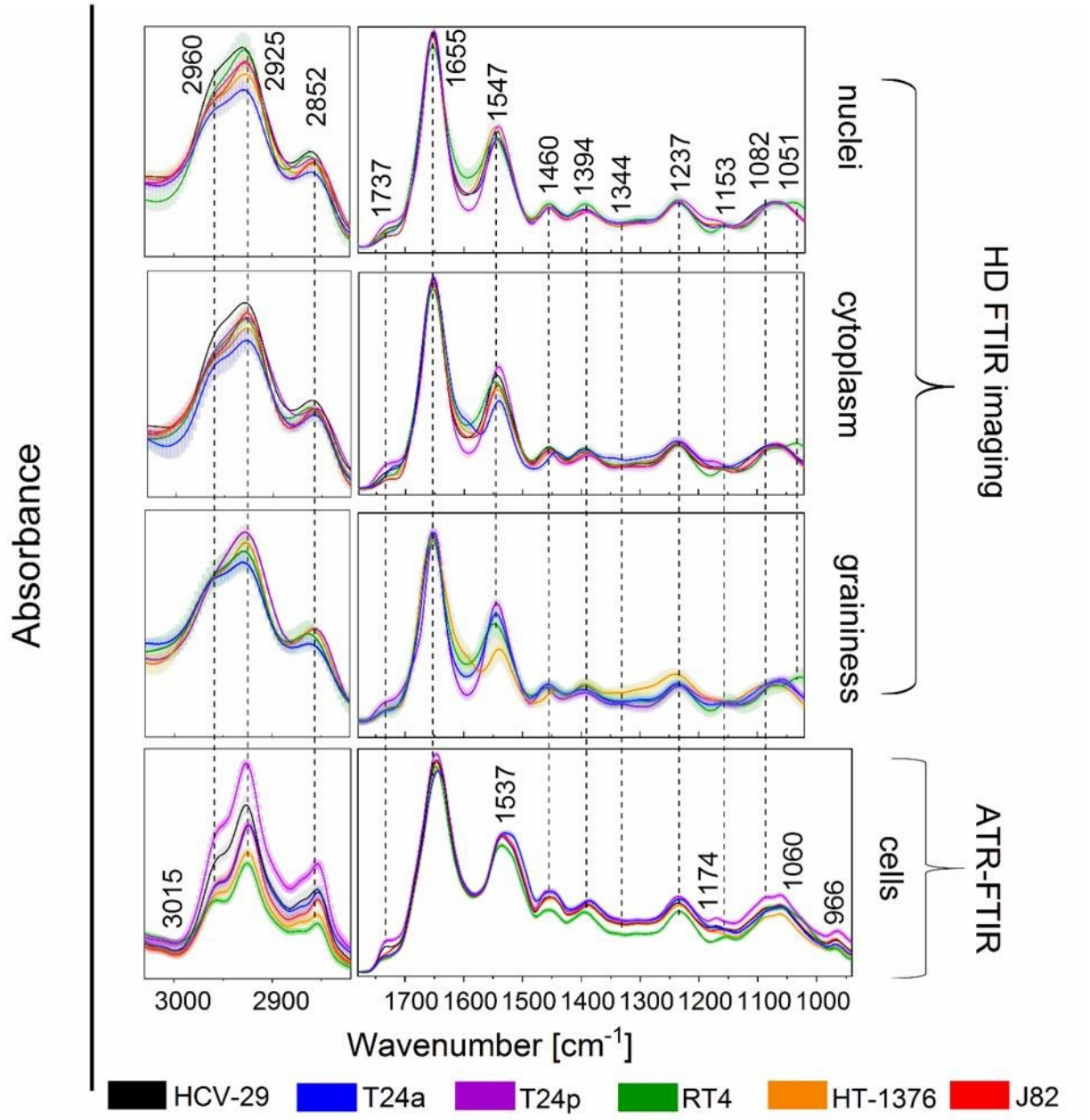

Figure S3. Averaged FTIR-transmission spectra of nuclei, cytoplasm and graininess and ATR-FTIR spectra of cell sediments. Spectra of cellular compartments were extracted from UHCA analysis of HD FTIR images. Gray shading denotes standard deviation (±SD).

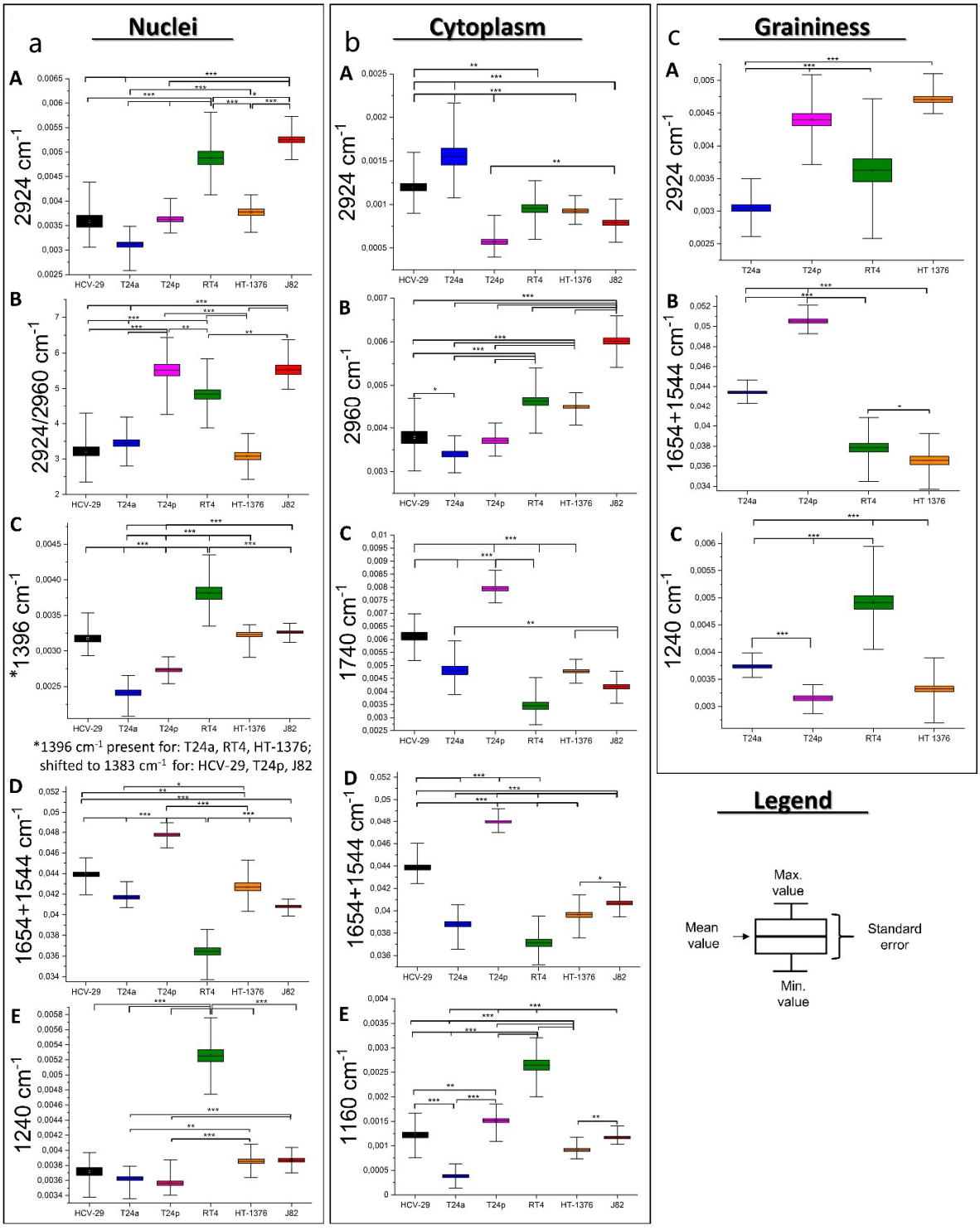

Figure S4. Changes in integral intensities of selected HD FTIR bands of cellular compartments.

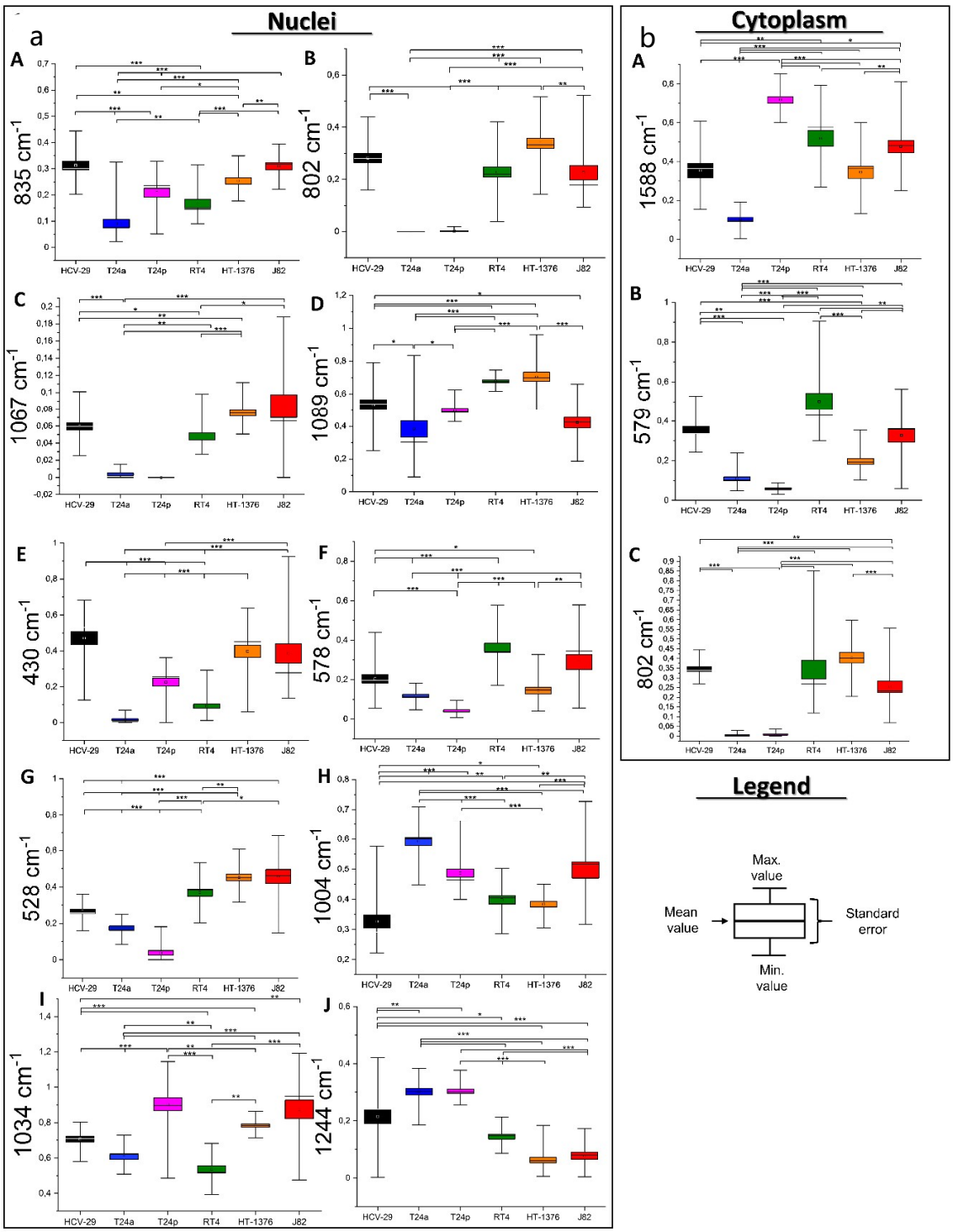

Figure S5. Changes in integral intensities of selected Raman bands of cellular compartments.

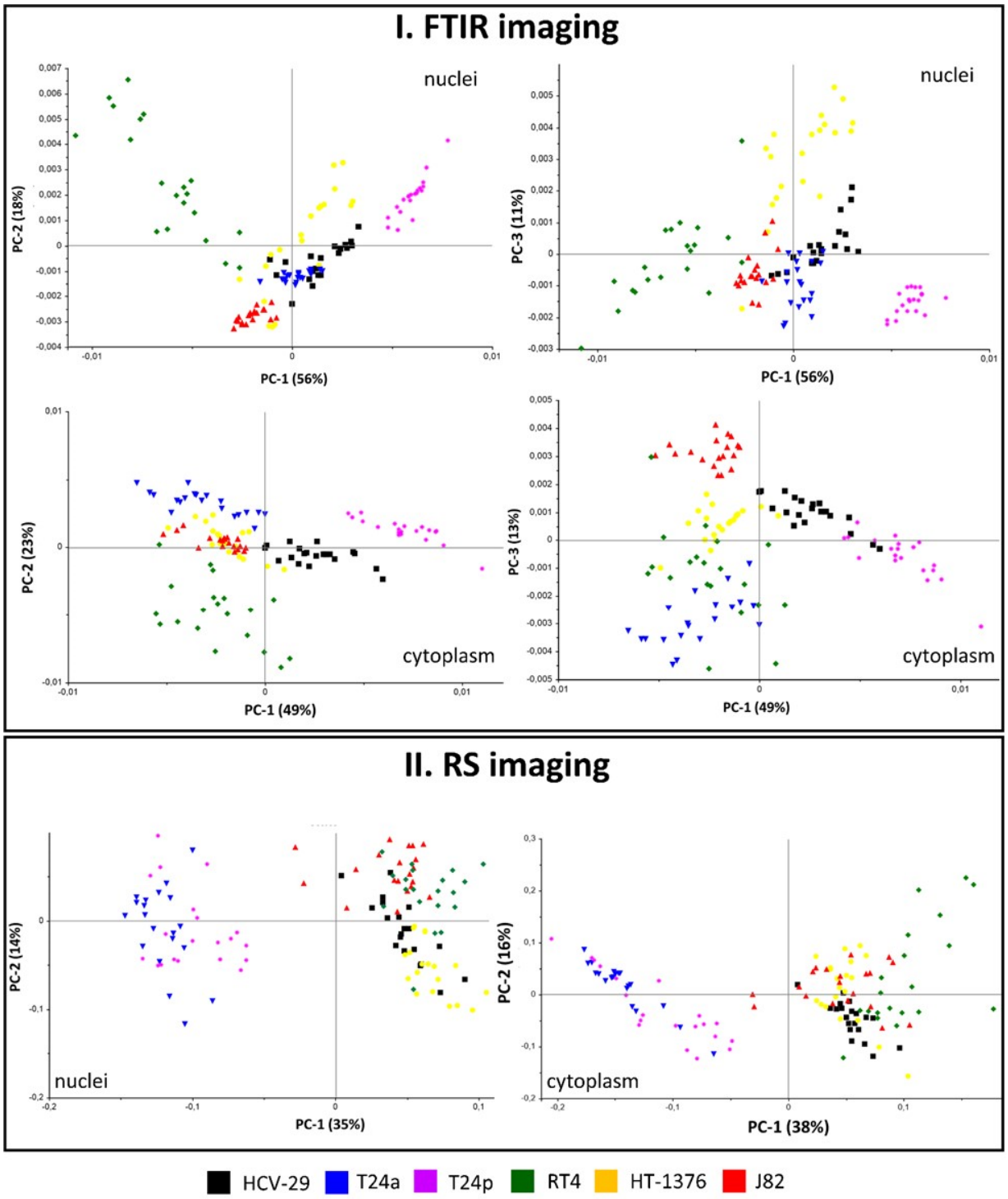

Figure S6. 2-dimensional score plots of PCA analysis displayed in Figure 6.

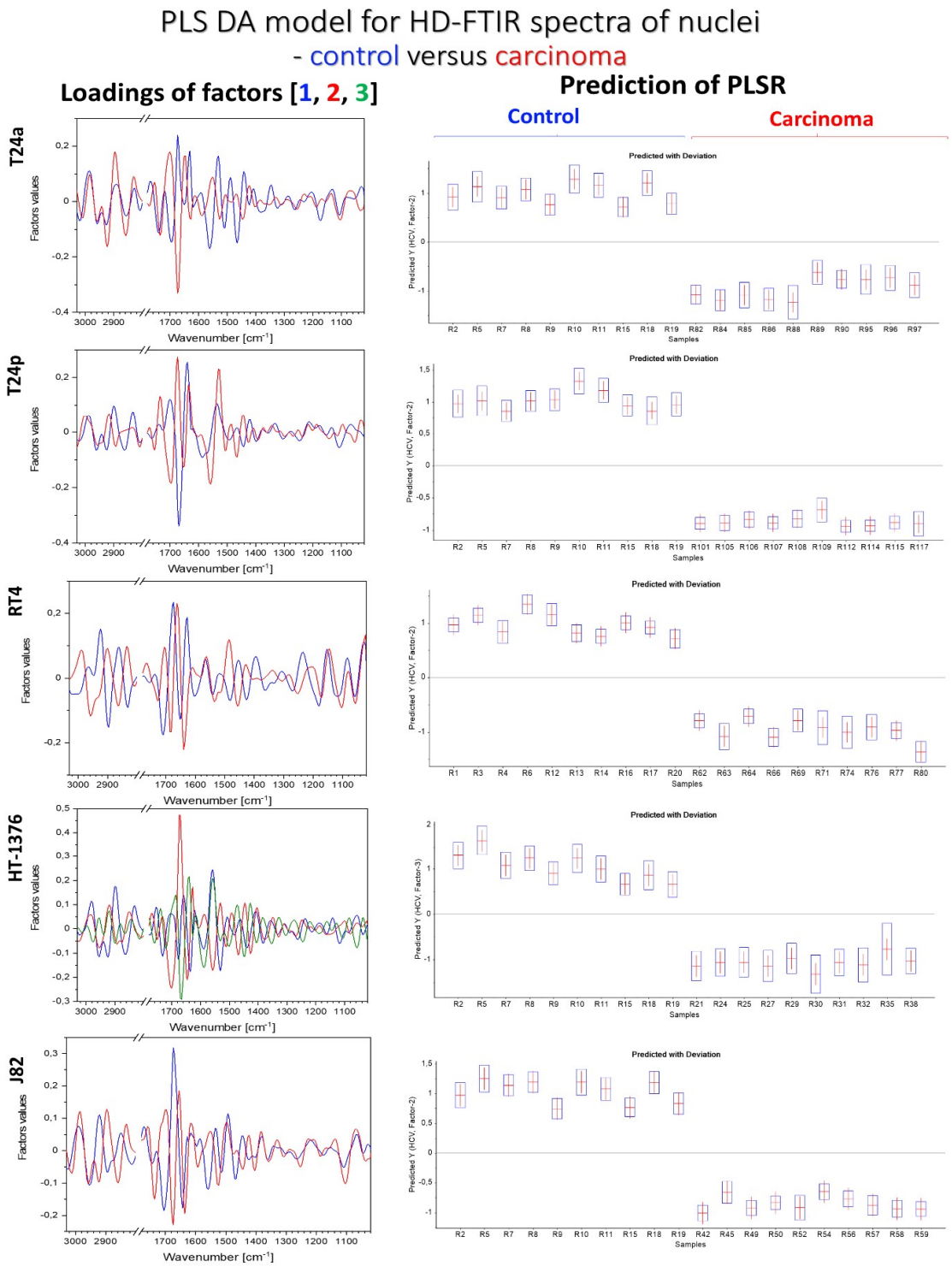

Figure S7. Partial Least Square Discrimination Analysis (PLS DA) of carcinoma and normal cells based on HD-FTIR spectra of nuclei.

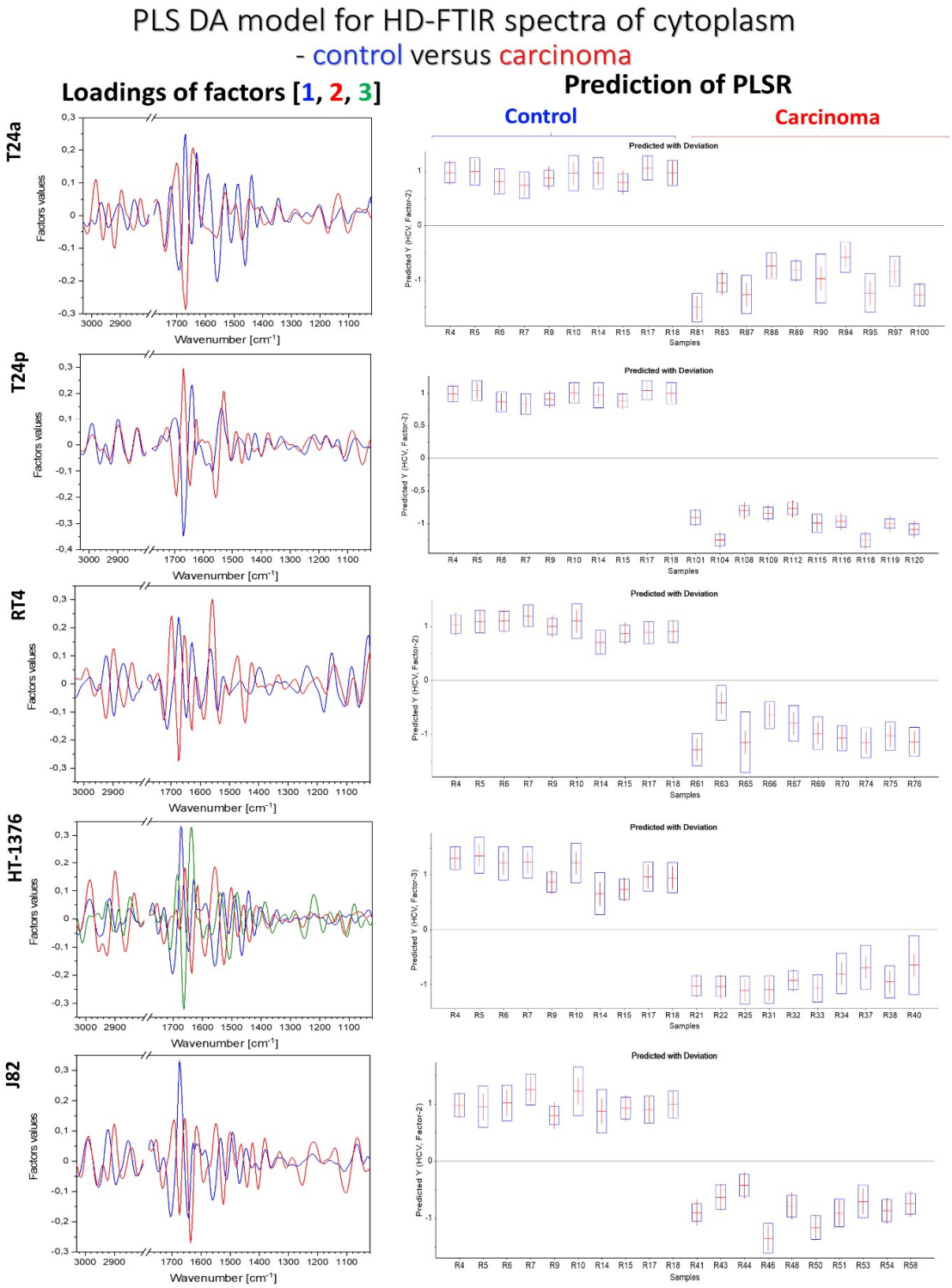

Figure S8. Partial Least Square Discrimination Analysis (PLS DA) of carcinoma and normal cells based on HD-FTIR spectra of cytoplasm.

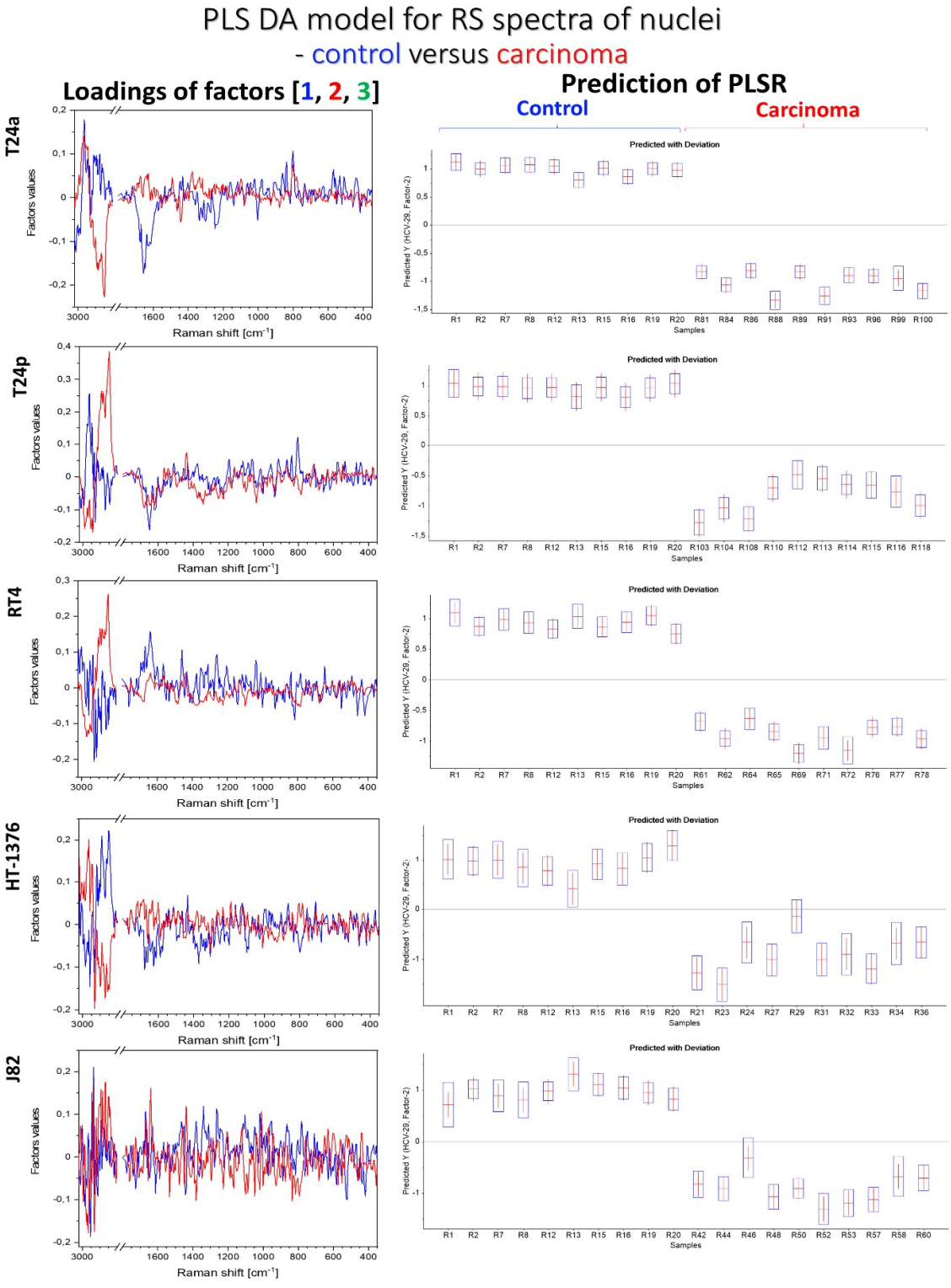

Figure S9. Partial Least Square Discrimination Analysis (PLS DA) of carcinoma and normal cells based on Raman spectra of nuclei.

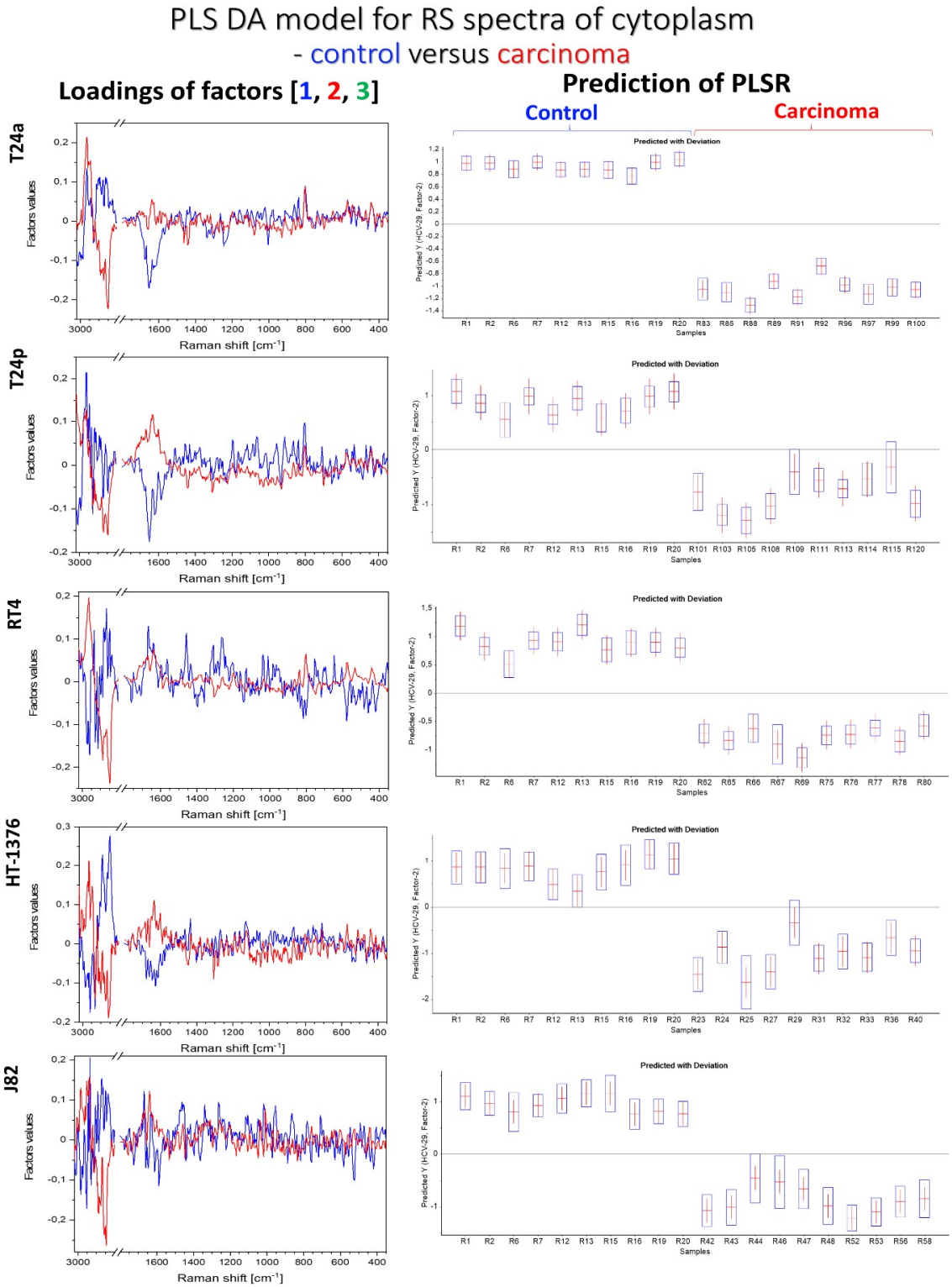

Figure S10. Partial Least Square Discrimination Analysis (PLS DA) of carcinoma and normal cells based on Raman spectra of cytoplasm.

Table S1. FTIR band positions observed in infrared spectra of the urothelial lines with their assignment to vibrational modes and biomolecules [1 – 5].

Position [cm^{-1}]	**Assignment to biomolecules and vibrational modes**
922	Carbohydrates; ν(C–C), ν(C–O)
966	DNA; ν(C-C)
996	RNA; Ring stretch and deformation of uracil
1022-1041	Carbohydrates, glycogen; ν(C–O)
1054	Carbohydrates, glycoproteins, glycolipids; ν(C–O) Nucleic acids; backbone ν(C–O) Cholesterol; ν(C–O)
1081	Nucleic acids; $\nu_s(PO_2^-)$ Phospholipids; $\nu_s(PO_2^-)$ Glycogen; ν(C-C)
1125	Ribose (RNA); ν(C-O) Polysaccharides; ν(CC-OC)
1153	Glycogen; ν_{as}(CO-O-C) Polysaccharides; ν_{as}(CO-O-C)
1160	Fatty acids and cholesterol esters; ν(C-O)
1240	Nucleic acids, phospholipids, phosphoproteins; $\nu_{as}(PO_2^-)$
1282	Proteins (amide III); ν(C-N) and ν(C-C)
1309	Proteins (amide III); ν(C-N) and ν(C-C)
1344	Phospholipids, fatty acids, triglycerides; $\delta(CH_2)$ Amino acid side chains; $\delta(CH_2)$
1396	Free fatty acids; $\nu_s(COO^-)$ Free amino acids; $\nu_s(COO^-)$
1445	Lipids; $\delta(CH_2, CH_3)$
1461	Proteins; $\delta(CH_2, CH_3)$ C (DNA); δ(NH), ν(CC)
1518	Tyr (proteins); ν(CC) of the Tyr ring C (methylated DNA); in-plane vibrations of the ring
1544	Proteins (amide II); δ(N-H) and ν(C-N)
1586	G (DNA); ν(C=C-C) of ring

1595	Free amino acids; $\nu_{as}(COO^-)$
1648-1654	α-Helices in proteins (amide I); ν(C=O) and δ(N-H)
1682	β-turns in proteins (amide I); ν(C=O) and δ(N-H) G (DNA); ν(C=O) and ν(C=C)
Position [cm^{-1}]	**Assignment to biomolecules and vibrational modes**
1718	Fatty acids; ν(C=O) Base pair (B-DNA); ν(C=O)
1735	Cholesterol esters; ν_{ester}(C=O)
1740	Triacylglycerols; ν_{ester}(C=O)
2850	Long chain fatty acids; $\nu_s(CH_2)$
2875	Proteins, lipids, nucleic acids; $\nu_s(CH_3)$
2895	Terminal CH_3 group in acyl chains (lipids); ν(CH)
2924	Lipids and proteins; $\nu_{as}(CH_2)$
2960	Proteins, lipids; $\nu_{as}(CH_3)$
3014	Unsaturated fatty acids; ν(=C-H)

ν – stretching mode, as – asymmetric, s – symmetric; δ – in-plane deformations; G – guanine; C – cytosine; Tyr – tyrosine.

Table S2. RS band positions observed in Raman spectra of the urothelial lines with their assignment to vibrational modes and biomolecules [6 – 11].

Position [cm^{-1}]	Assignment to biomolecules and vibrational modes
430	Cholesterol, cholesterol esters
528	*ggt* conformation of S-S bonds in proteins; ν(S-S)
579	Carbohydrates, Trp; δ(C-C=O)
609	Cholesterol, cholesterol esters; ν(steroid ring)
647	Tyr
701	Cholesterol, cholesterol esters; ν(steroid ring)
722	A (nucleic acids); ring breathing Phospholipids Proteins; ν(C-S)
751	Cyt. c, c_1 and b; ν_{15}, ν_s(pyr deform)sym
785	DNA; ν_{as}(OPO) U, T, C (nucleic acids)
802	Phospholipids; ν(OPO) Nucleic acids; δ(CH-CHO)
835	Tyr (proteins); ring breathing DNA; ν_s(OPO) DNA B Glucose; ν(C-C) and ν(C-O-C-O)
860	Tyr (proteins); ν_s(C-C-N^+)

Position [cm^{-1}]	Assignment to biomolecules and vibrational modes
893	Trp (proteins); ν(C-C) and ν(C-N)
930	Cholesterol esters (lipid droplets); ν(C-C)
935	Protein (keratin like structure in uroplakin); ν(C-C)
962	Carbohydrates; ν(C-O) Nucleic acids; phosphodiester chain
1004	Phe (proteins); ring breathing
1034	Proteins crosslinking; δ(C-H) and δ(C-N)
1067	Lipids (*gauche* in acyl backbone); ν(C-C)

1089	Phospholipids; ν(PO_2^-) Lipids (*trans* in acyl backbone); ν(C-C)
1129	Lipids (*trans* in acyl backbone); ν(C-C) Cyt; ν(C-N) Proteins; ν(C-O) Carbohydrates; ν(C-O)
1179	Tyr, Phe (proteins); δ(C-H) C, G (nucleic acids); ν(C-C)
1209	Tyr, Phe, Trp, Hyp (proteins); τ(CH_2)
1244	Amide III (likely uroplakin); ν(C-N) and δ(N-H)
1268	Amide III; ν(C-N) and δ(N-H) Lipids; δ(=CH)
1280	Lipids; δ(CH_2)
1307	Lipids; τCH_2-CH_3
1344	A (nucleic acids); δ(CH) Proteins; δ(CH) Carbohydrates; δ(CH) Reduced cyt. b
1375	A (nucleic acids); δ(CH_3)
1447	Proteins, lipids; δ(CH_2), δ(CH_3)
1588	Reduced cyt. c and b
1660	Proteins (amide I); ν(C=O) and δ(N-H) Unsaturated fatty acids; ν(C=C)
1725	Cholesterol esters; ν_{ester}(C=O)
1737	Triacylglycerols, ν_{ester}(C=O)
2852	Long chain fatty acids; ν_s(CH_2)
2875	Lipids, proteins; ν(C-H)-CH_2
2893	Lipids, proteins; ν_s(-C-H)-CH_3
Position [cm^{-1}]	**Assignment to biomolecules and vibrational modes**
2935	Lipids, proteins; ν(C-H)
2962	Nucleic acids, lipids; ν_{as}(CH_3), ν_{as}CH(-CH_2)

3015	Unsaturated fatty acids; ν(=C-H)

ν – stretching mode, as – asymmetric, s – symmetric; δ – in-plane deformations; τ – twisting; cyt – cytochromes; A – adenine; C – cytosine, G – guanine; U – uracil; T – thymine; Tyr – tyrosine; Phe – phenylalanine; Trp – tryptophan; Hyp – proline.

Table S3. PLS-DA parameters for discrimination of carcinoma (T24a, T24p, TR4, HT-1376, and J82) and normal urothelial cells (HCV-29) obtained for IR and Raman spectra of nuclei and cytoplasm.

Cancer cell line	**T24a**	**T24p**	**RT4**	**HT-1376**	**J82**
PLS parameters	**RMSE / R^2**	**RMSE / R^2**	**RMSE / R^2**	**RMSE / R^2**	**RMSE / R^2**
HD-FTIR spectra of nuclei					
Calibration	0.23 / 0.95	0.17 / 0.97	0.19 / 0.96	0.30 / 0.91	0.17 / 0.97
Validation	0.33 / 0.90	0.23 / 0.95	0.23 / 0.95	0.46 / 0.81	0.24 / 0.95
Prediction	0.21 / 0.96	0.14 / 0.98	0.19 / 0.96	0.24 / 0.94	0.19 / 0.97
HD-FTIR spectra of cytoplasm					
Calibration	0.22 / 0.95	0.13 / 0.98	0.27 / 0.93	0.16 / 0.97	0.20 / 0.96
Validation	0.28 / 0.93	0.16 / 0.98	0.35 / 0.89	0.33 / 0.90	0.27 / 0.93
Prediction	0.22 / 0.95	0.13 / 0.98	0.21 / 0.96	0.21 / 0.96	0.23 / 0.95
RS spectra of nuclei					
Calibration	0.12 / 0.99	0.19 / 0.96	0.15 / 0.98	0.29 / 0.91	0.16 / 0.97
Validation	0.16 / 0.98	0.25 / 0.94	0.22 / 0.96	0.43 / 0.83	0.30 / 0.92
Prediction	0.14 / 0.98	0.23 / 0.95	0.17 / 0.97	0.32 / 0.90	0.24 / 0.94
RS spectra of cytoplasm					
Calibration	0.10 / 0.99	0.20 / 0.96	0.20 / 0.96	0.34 / 0.88	0.21 / 0.95
Validation	0.15 / 0.98	0.26 / 0.94	0.28 / 0.93	0.47 / 0.80	0.37 / 0.87
Prediction	0.14 / 0.98	0.89 / 0.89	0.25 / 0.94	0.33 / 0.89	0.22 / 0.95

References

1. Sahu, R.K.; Argov, S.; Salman, A.; Huleihel, M.; Grossman, N.; Hammody, Z.; Kapelushnik, J.; Mordechai, S Mordechai. Characteristic absorbance of nucleic acids in the Mid-IR region as possible common biomarkers for diagnosis of malignancy. *Technol. Cancer Res. Treat.* **2004**, *3*, 629–638.
2. Staniszewska, E.; Malek, K.; Baranska, M. Rapid approach to analyze biochemical variation in rat organs by ATR FTIR spectroscopy. *Spectrochim. Acta - Part A Mol. Biomol. Spectrosc.* **2014**, *118*, 981–986.
3. Wiercigroch, E.; Staniszewska-Slezak, E.; Szkaradek, K.; Wojcik, T.; Ozaki, Y.; Baranska, M.; Malek, K. FT-IR Spectroscopic Imaging of Endothelial Cells Response to Tumor Necrosis Factor-α: To Follow Markers of Inflammation Using Standard and High-Magnification Resolution. *Anal. Chem.* **2018**, *90*, 3727–3736.
4. Banyay, M.; Sarkar, M.; Gräslund, A. A library of IR bands of nucleic acids in solution. *Biophys. Chem.* **2003**, *104*, 477–488.
5. Whelan, D.R.; Bambery, K.R.; Heraud, P.; Tobin, M.J.; Diem, M.; McNaughton, D.; Wood, B.R. Monitoring the reversible B to A-like transition of DNA in eukaryotic cells using Fourier transform infrared spectroscopy. *Nucleic Acids Res.* **2011**, *39*, 5439–5448.
6. Bik, E.; Dorosz, A.; Mateuszuk, L.; Baranska, M.; Majzner, K. Fixed versus live endothelial cells: The effect of glutaraldehyde fixation manifested by characteristic bands on the Raman spectra of cells. *Spectrochim. Acta - Part A Mol. Biomol. Spectrosc.* **2020**, *240*, 118460.
7. Majzner, K.; Chlopicki, S.; Baranska, M. Lipid droplets formation in human endothelial cells in response to polyunsaturated fatty acids and 1-methyl-nicotinamide (MNA); confocal Raman imaging and fluorescence microscopy studies. *J. Biophotonics* **2016**, 9, 396–405.
8. Prescott, B.; Steinmetz W.; Thomas, G. J. Characterization of DNA structures by laser Raman spectroscopy. *Biopolymers* **1984**, *23*, 235–256.
9. Brazhe, N.A.; Treiman, M.; Brazhe, A. R.; Find, N.L.; Maksimov, G.V.; Sosnovtseva, O.V. Mapping of Redox State of Mitochondrial Cytochromes in Live Cardiomyocytes Using Raman Microspectroscopy. *PLoS One* **2012**, *7*, 1–8.
10. Harvey, T.J.; Hughes, C.; Ward, A.D.; Faria, E.C.; Henderson, A.; Clarke, N.W.; Brown, M.D.; Snook, R.D.; Gardner P. Classification of fixed urological cells using Raman tweezers. *J. Biophotonics*. **2009**, 2, 47–69.
11. Jen, C.P.; Huang, C. Te.; Chen, Y.S.; Kuo C.T.; Wang, H. C. Diagnosis of human bladder cancer cells at different stages using multispectral imaging microscopy. *IEEE J. Sel. Top. Quantum Electron.* **2014**, *20*, 6800808.